Molecular Therapy
Original Article

MicroRNA-34a Promotes Renal Fibrosis by Downregulation of Klotho in Tubular Epithelial Cells

Yong Liu,[1] Xianjin Bi,[1] Jiachuan Xiong,[1] Wenhao Han,[1] Tangli Xiao,[1] Xinli Xu,[1] Ke Yang,[1] Chi Liu,[1] Wei Jiang,[1] Ting He,[1] Yanlin Yu,[1] Yan Li,[1] Jingbo Zhang,[1] Bo Zhang,[1] and Jinghong Zhao[1]

[1]Department of Nephrology, Institute of Nephrology of Chongqing and Kidney Center of PLA, Xinqiao Hospital, Third Military Medical University, Chongqing 400037, China

Renal fibrosis is the main pathological characteristic of chronic kidney disease (CKD), whereas the underlying mechanisms of renal fibrosis are not clear yet. Herein, we found an increased expression of microRNA-34a (miR-34a) in renal tubular epithelial cells of patients with renal fibrosis and mice undergoing unilateral ureteral obstruction (UUO). In miR-34a$^{-/-}$ mice, miR-34a deficiency attenuated the progression of renal fibrosis following UUO surgery. The miR-34a overexpression promoted epithelial-to-mesenchymal transition (EMT) in cultured human renal tubular epithelial HK-2 cells, which was accompanied by sharp downregulation of Klotho, an endogenous inhibitor of renal fibrosis. Luciferase reporter assay revealed that miR-34a downregulated *Klotho* expression though direct binding with the 3′ UTR of *Klotho*. Conversely, overexpression of *Klotho* prevented miR-34a-induced EMT in HK-2 cells. Furthermore, results showed that miR-34a was induced by transforming growth factor β1 (TGF-β1) through p53 activation, whereas dihydromyricetin could inhibit TGF-β1-induced miR-34a overexpression. Accordingly, dihydromyricetin administration dramatically restored the aberrant upregulation of miR-34a and Klotho reduction in obstructed kidney, and markedly ameliorated renal fibrosis in the Adriamycin nephropathy and UUO model mice. These findings suggested that miR-34a plays an important role in the progression of renal fibrosis, which provides new insights into the pathogenesis and treatment of CKD.

INTRODUCTION

The incidence of chronic kidney disease (CKD) is a worldwide problem that seriously threatens human health and has increased annually.[1–3] In CKD patients, regardless of the initial etiology, renal fibrosis is the predominant cause of renal function loss and is considered as a critical pathological characteristic leading to end-stage renal disease (ESRD).[4–6] Renal fibrosis is characterized by increased production of α-smooth muscle actin (α-SMA) and extracellular matrix (ECM) in the interstitium.[7,8] Although it has been demonstrated that tubular epithelial cells plasticity and interstitial fibroblast proliferation are two major contributors to renal fibrosis,[9] the molecular mechanisms of renal fibrosis have not been fully elucidated yet.

MicroRNAs (miRs) are small, noncoding RNAs that directly bind to the 3′ UTR of target mRNAs and negatively regulate the gene expression.[10,11] The miRs plays crucial roles in diverse biological processes, including cell development, differentiation, and survival.[12–14] Aberrant miR expressions were found to be correlated with inflammatory diseases, metabolic diseases, cancers, and many more.[15–17] Several miRs are involved in the progression of a variety of kidney diseases, including renal cell carcinomas,[18] diabetic nephropathy,[19] and acute kidney injury (AKI).[20] miR-34a is a transcriptional target of p53, which regulates the cell cycle and apoptosis, but the deficiency of the miR-34a may contribute to cancer cell proliferation and resistance to various therapies.[21] Notably, recent studies showed that expression of miR-34a was upregulated in renal tubular cells in mice with cisplatin-induced nephrotoxicity.[22] However, the distinct roles of miR-34a in renal fibrosis are still not well clarified.

Dihydromyricetin (DHM), a 2,3-dihydroflavonol compound, is a kind of natural flavonoid extracted from the Chinese herb *Ampelopsis grossedentata*, which is a popular and multipurpose traditional Chinese medicinal herb and has been used as herbal medicine or health tea (Tengcha).[23] It has been reported that DHM displays a broad range of biological and pharmacological activities, including strong anti-inflammatory, antibacterial, and antitumor properties, antioxidant properties, and neuroprotective and hepatoprotective effects, making it beneficial for the amelioration of atherosclerosis, attenuation of diabetic cardiomyopathy, and induction of cancer cells apoptosis.[24–26] As known, tubular interstitial fibrosis is a hallmark of kidney aging, and inflammation and oxidative stress play important roles in the development of renal fibrosis.[27,28] All of these

Received 26 August 2018; accepted 6 February 2019;
https://doi.org/10.1016/j.ymthe.2019.02.009.

Correspondence: Jinghong Zhao, Department of Nephrology, Institute of Nephrology of Chongqing and Kidney Center of PLA, Xinqiao Hospital, Third Military Medical University, Chongqing 400037, China.
E-mail: zhaojh@tmmu.edu.cn

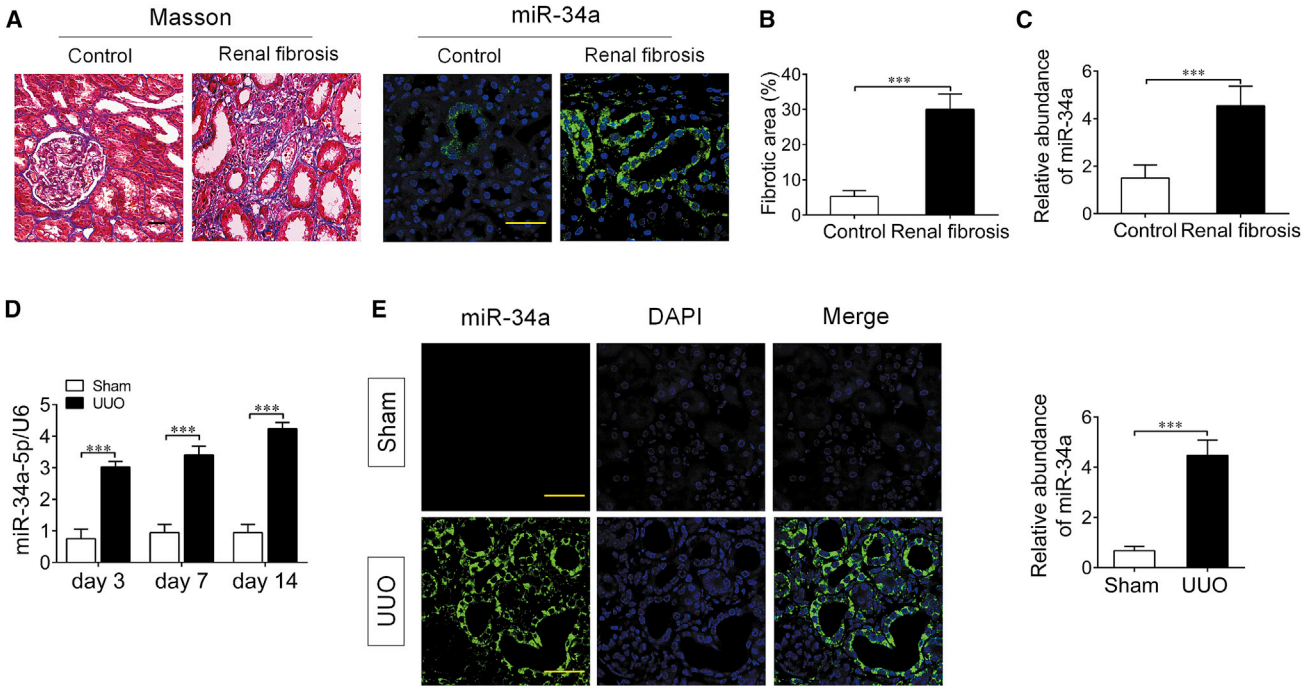

Figure 1. miR-34a Expression Was Significantly Upregulated in the Kidney of Patients with Renal Fibrosis and UUO Mice

(A) Representative micrographs of Masson trichrome and fluorescence *in situ* hybridization of miR-34a in kidney tissue biopsy samples from patients with renal fibrosis (n = 8) and control patients (n = 5). Paraffin sections were used for Masson trichrome staining and *in situ* hybridization. (B) Graphical presentation of kidney fibrotic lesions in different groups after quantitative determination. The fibrotic lesions were indicated by blue areas in the center. (C) Quantification of miR-34a in kidney tissue biopsy samples in patients with renal fibrosis. (D) The expression of miR-34a was determined by qRT-PCR in the mouse obstructed kidney at 3, 7, and 14 days after UUO surgery. U6 was used for normalization. (E) Representative images showing the expression and localization of miR-34a at 14 days after UUO surgery by *in situ* hybridization. Quantification of miR-34a in the mouse obstructed kidney at 14 days after UUO surgery. The scale bar corresponds to 50 μm. Data are means ± SD. n = 6 mice per group. ***$p < 0.001$.

findings prompt us to hypothesize that DHM may also have therapeutic potential against renal fibrosis.

Herein, our study showed that miR-34a expression was upregulated in tubular epithelial cells in patients with renal fibrosis and in obstructed kidney in unilateral ureteral obstruction (UUO) mice. Moreover, it is also revealed that miR-34a promoted tubular interstitial fibrosis at least in part due to its downregulation of Klotho, an endogenous inhibitor of pro-fibrotic signaling pathways. We further found that DHM was able to increase Klotho expression and executed inhibitory effect on renal fibrosis through suppressing miR-34a upregulation. These findings will provide new insights into the pathogenesis and therapeutic target of renal fibrosis, and pioneer to demonstrate that DHM may be a potential natural medicine to treat CKD.

RESULTS

Renal miR-34a Expression Increases Significantly in Both Patients with Renal Fibrosis and UUO Mice

To investigate the role of miR-34a in the pathogenesis of CKD, we first conducted immunostaining in kidney biopsy specimens from patients with renal fibrosis (Table S1). A significant increase in the expression of miR-34a was obviously observed in biopsy samples of fibrotic kidneys from patients with renal fibrosis. Notably, miR-34a expression was predominantly localized in the renal tubular epithelium of fibrotic kidneys (Figures 1A–1C). We further examined the expression changes of miR-34a during the progression of renal fibrosis in UUO mice and found that the expression level of miR-34a increased progressively after obstructed injury and reached maximal point at 14 days (Figure 1D). The increased expression of miR-34a was also mainly found in tubular cells in the obstructed kidney in UUO mice (Figure 1E). Taken together, these findings suggest that miR-34a expression was upregulated during the progression of renal fibrosis.

miR-34a Deficiency Ameliorates Renal Fibrosis in UUO Mice

Based on the finding that miR-34a was aberrantly upregulated in the progression of renal fibrosis, we thought that miR-34 might contribute to renal fibrosis. To confirm it, we used miR-34a knockout (miR-34a$^{-/-}$) mice for further investigation. As shown in Figure 2A, miR-34a is deficient in miR-34a$^{-/-}$ mice. Masson staining revealed that the expansion of interstitial area was dramatically attenuated in miR-34a$^{-/-}$ UUO mice, compared with that in wild-type (WT) UUO mice (Figure 2B). Meanwhile, a significant decrease in E-cadherin (tubular epithelial marker) expression and remarkable increases in serum creatinine and blood urea nitrogen level, as well as α-SMA and fibronectin expressions, were found in the obstructed kidney in WT UUO mice at 14 days after surgery, whereas all of these changes

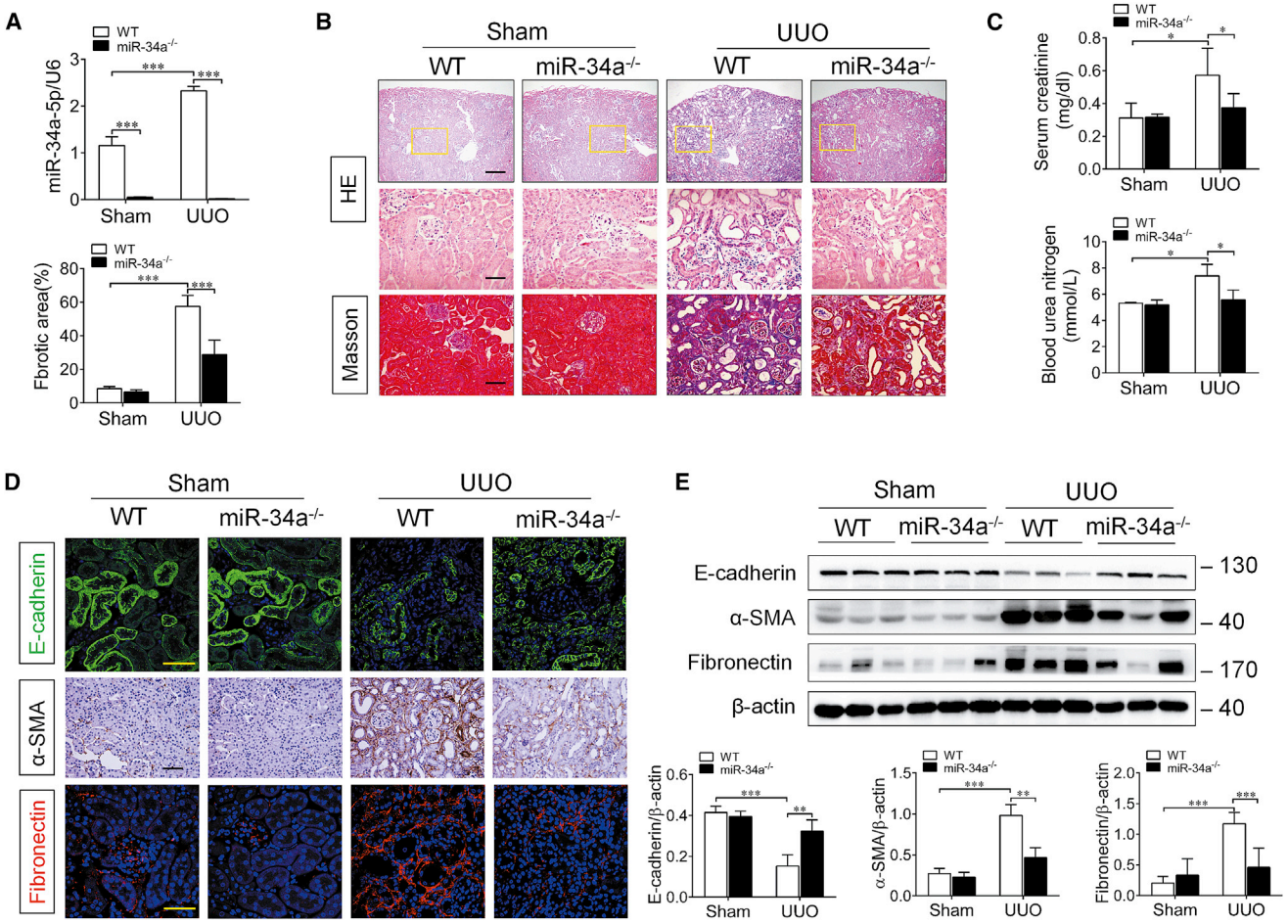

Figure 2. miR-34a Deficiency Ameliorated Renal Fibrosis in UUO Mice

(A) qRT-PCR analysis of miR-34a expression in the mouse obstructed kidney at 14 days after UUO surgery. (B) Representative micrographs of H&E and Masson trichrome-stained kidney sections of mice at 14 days after UUO surgery. Paraffin sections were used for H&E and Masson trichrome staining. The fibrotic lesions were indicated by blue areas in the center. Graphical presentation of kidney fibrotic lesions in different groups after quantitative determination. The top scale bar corresponds to 200 μm; the center and bottom scale bars correspond to 50 μm. (C) Serum creatinine and blood urea nitrogen levels were assessed at 14 days after UUO surgery. (D) Representative immunostaining of E-cadherin, α-SMA, and fibronectin in the mouse obstructed kidney at 14 days after UUO surgery. E-cadherin (green), fibronectin (red), and DAPI (blue). The scale bar corresponds to 50 μm. (E) Western blotting analysis for E-cadherin, α-SMA, and fibronectin protein levels in UUO mice at 14 days after surgery. Data are means ± SD. n = 6 mice per group. ***$p < 0.001$, **$p < 0.01$.

were alleviated in miR-34a$^{-/-}$ UUO mice (Figures 2C–2E). These data indicate that miR-34a upregulation contributes to renal fibrosis in UUO mice.

miR-34a Upregulation Induces Tubular Epithelial Cells Plasticity through Downregulation of Klotho

To further determine the effect of miR-34a upregulation on renal fibrosis, human proximal tubule epithelial HK-2 cells were transfected with a miR-34a mimic, and the tubular epithelial cells plasticity was assessed. Our results showed that overexpression or knockdown of miR-34a with mimic or inhibitor had no obvious effect on the cell viability of HK-2 cells (Figure S1A). As shown in Figure 3A, miR-34a expression was markedly elevated in HK-2 cells after transfection with miR-34a mimic, but not miR-negative control. Consequently, miR-34a mimic transfection significantly suppressed E-cadherin expression and increased the expressions of α-SMA and fibronectin (Figure 3B). Immunofluorescence staining revealed that the expression of α-SMA was increased in HK-2 cells after miR-34a mimic transfection (Figure 3C), suggesting that miR-34a overexpression can induce tubular epithelial cells transition into a pro-fibrotic phenotype.

Next, we investigated the mechanisms underlying the effect of miR-34a-induced tubular epithelial cells plasticity. By using bioinformatics analysis, we found that there existed imperfect complementary sequences between miR-34a and the 3′ UTR of mouse or human *Klotho* mRNA (Figure 3D). Because Klotho was reported to be an important endogenous inhibitor of tubular interstitial fibrosis,[29] we wondered whether Klotho might be a potential target of miR-34a. As expected,

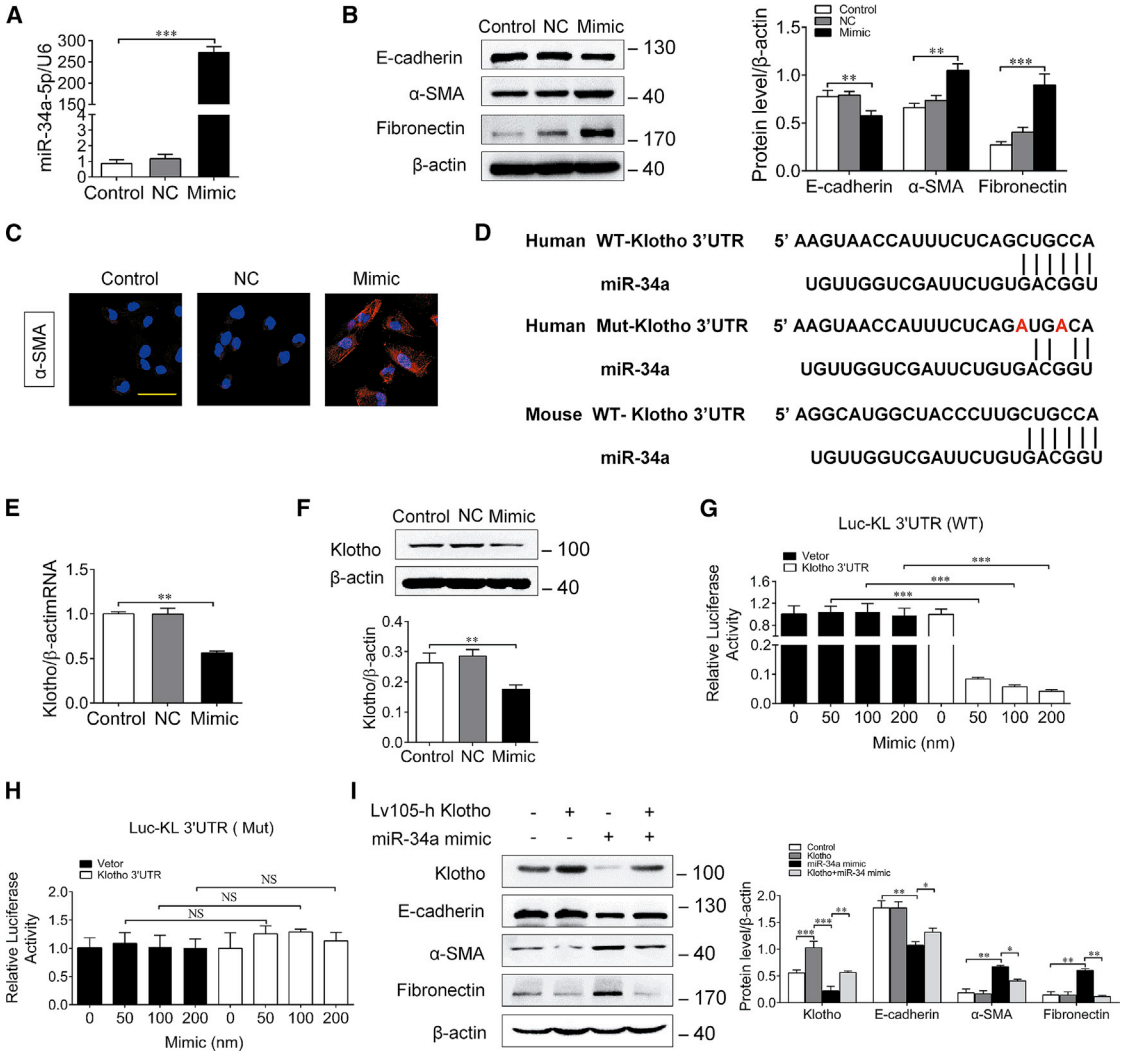

Figure 3. miR-34a Upregulation Induced Tubular Epithelial Cells Plasticity and Downregulation of Klotho

(A) qRT-PCR analysis of miR-34a expression in HK-2 cells transfected with miR-34a mimic (100 nM) or a miR-negative control for 48 h. (B) Representative immunostaining of E-cadherin, α-SMA, and fibronectin in HK-2 cells transfected with an miR-34a mimic (100 nM) or an miR-negative control for 48 h. (C) Representative immunostaining of α-SMA in HK-2 cells transfected with miR-34a mimic (100 nM) or a miR-negative control for 48 h. (D) Schematic of the Klotho 3′ UTR with the WT or mutated putative binding site of miR-34a inserted into a luciferase (Luc) reporter. (E) qRT-PCR analysis of Klotho mRNA expression in HK-2 cells transfected with miR-34a mimic for 48 h. (F) Western blot analysis of Klotho in HK-2 cells transfected with miR-34a mimic for 48 h. (G and H) Relative luciferase activity in HK2 cells that are cotransfected with plasmids containing firefly luciferase and (G) wild-type (WT) or (H) mutant (Mut) human of Klotho 3′ UTR and miR-34a mimic or miR-negative control for 48 h. The values for luciferase activities were normalized to Renilla reniformis luciferase (TK-RL) activities. (I) Western blot analysis of E-cadherin, α-SMA, and fibronectin in HK-2 cells cotransfected with miR-34a mimic and Klotho for 48 h. The scale bar corresponds to 50 μm. Data are means ± SD. ***p < 0.001, **p < 0.01, *p < 0.05. NS, statistically nonsignificant.

the expression of Klotho declined significantly both at mRNA and protein levels in HK-2 cells after transfection with miR-34a mimic (Figures 3E and 3F). To examine whether miR-34a could directly target *Klotho* mRNA, a luciferase reporter inserted with a WT or mutated putative binding site of miR-34a in the 3′ UTR of *Klotho* gene was constructed and transfected into HK-2 cells. Inspiringly, miR-34a mimic could dose-dependently inhibit the luciferase activity of the WT-*Klotho* reporter (Figure 3G), but it displayed no obvious effect on the activity of Mutant-*Klotho* reporter (Figure 3H). Conversely, overexpression of Klotho significantly prevented the increased expressions of α-SMA and fibronectin, and decreased expression of E-cadherin induced by miR-34a mimic in HK-2 cells (Figure 3I). These data suggest that miR-34a-induced tubular epithelial cells plasticity is at least in part due to its direct downregulation of Klotho.

miR-34a Upregulation Induces Klotho Reduction and Activates Pro-fibrotic Signal Pathways in UUO Mice

Subsequently, we detected the *in vivo* effect of miR-34a on Klotho expression during the progression of renal fibrosis in UUO mice. For this purpose, we determined and compared the expression level

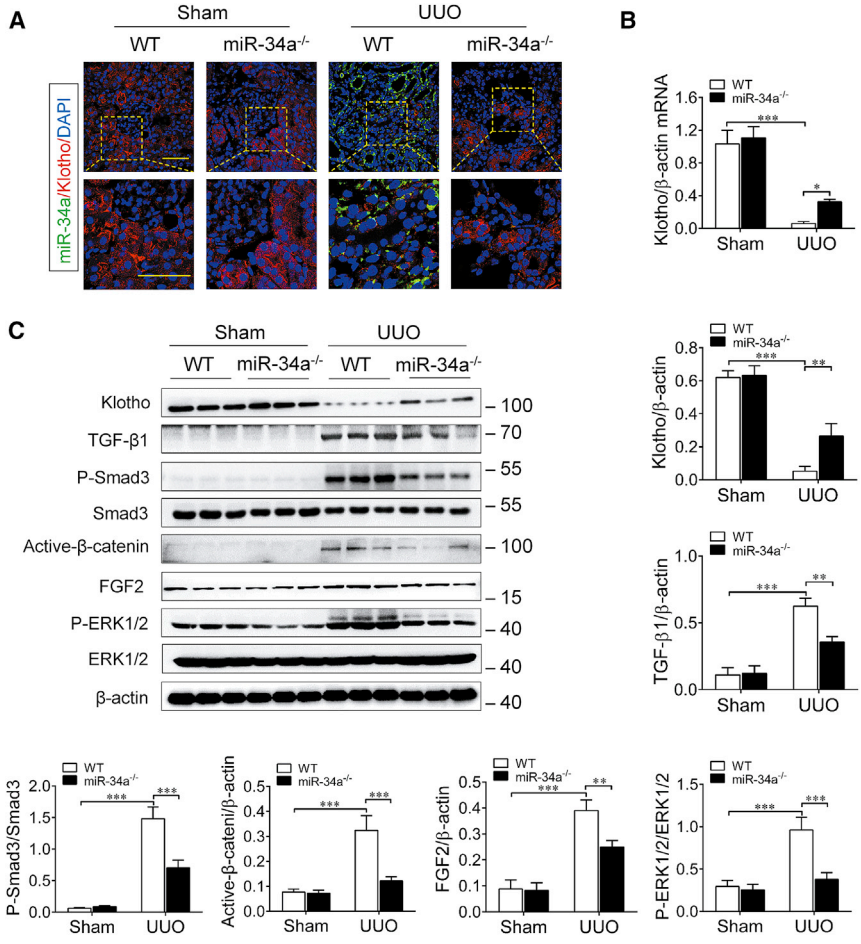

Figure 4. miR-34a Knockout Retained Klotho Expression and Inhibited Pro-fibrotic Signal Pathway Activation in UUO Mice

(A) Representative immunofluorescence of double-immunofluorescence staining with *in situ* hybridization (probe against miR-34a) and immunofluorescence (antibody against Klotho) in the mouse obstructed kidneys at 14 days after UUO surgery. The scale bars correspond to 50 μm. (B) qRT-PCR analysis of Klotho mRNA expression in the mouse obstructed kidney at 14 days after UUO surgery. (C) Western blotting analysis for Klotho, TGF-β1, phospho-smad3, active-β-catenin, FGF2, and phospho-ERK1/2 protein levels in UUO mice at 14 days after surgery. Data are means ± SD. n = 6 mice per group. ***$p < 0.001$, **$p < 0.01$.

of Klotho in the obstructed kidney in WT UUO mice and miR-34a$^{-/-}$ UUO mice. As shown in Figure 4A, the expression of miR-34a (green) was obviously increased in the obstructed kidney in UUO mice, accompanied by a marked reduction of Klotho (red) as determined by double-immunofluorescence staining. However, we observed only a few co-stainings of miR-34a and Klotho in tubular epithelial cells because of diametrically opposed levels of expression. Similarly, higher mRNA level of *Klotho* was also detected in miR-34a$^{-/-}$ UUO mice by qRT-PCR assay (Figure 4B). Meanwhile, the increased expressions of pro-fibrotic factors, such as phospho-Smad3, active-β-catenin, and phospho-extracellular regulated protein kinase (ERK)1/2, downstream of transforming growth factor β1 (TGF-β1), Wnts, and fibroblast growth factor 2 (FGF2) were markedly attenuated in miR-34a$^{-/-}$ UUO mice, as compared with those in WT UUO mice (Figure 4C). These results demonstrate that miR-34a elevation can induce Klotho reduction and activations of pro-fibrotic signal pathways in the kidney after UUO injury.

TGF-β1 Induces the Upregulation of miR-34a in HK-2 Cells

As reported, TGF-β1 was recognized as a pivotal mediator of renal fibrosis, and previous studies revealed that TGF-β1 promoted renal fibrosis partly through regulation of miRs.[19,30–33] However, whether TGF-β1 is also a regulator of miR-34a in tubular epithelial cells is not clear. Interestingly, here we found that TGF-β1 could upregulate miR-34a expression in HK-2 cells in a dose- and time-dependent manner, and the effect was reversed by miR-34a inhibitor (Figures 5A–5C). Meanwhile, the Klotho expression was significantly suppressed by TGF-β1, and miR-34a inhibitor was able to eliminate TGF-β1-induced Klotho suppression (Figures 5D and 5E). In addition, miR-34a inhibitor also significantly attenuated TGF-β1-induced downregulation of E-cadherin and upregulations of α-SMA and fibronectin (Figure 5F). These findings indicate that miR-34a may be an important mediator of TGF-β1 in promoting pro-fibrotic phenotype transition in tubular epithelial cells.

DHM Inhibits TGF-β1-Induced Upregulation of miR-34a in HK-2 Cells

Because DHM was reported to be able to suppress miR-34a expression for the treatment of Alzheimer's disease in rats,[34] we then wonder whether DHM has the potential to inhibit miR-34a upregulation in tubular epithelial cells. To this end, HK-2 cells were stimulated with TGF-β1 with or without DHM for 24 or 48 h. First, the effect of DHM on cell viability was detected by Cell Counting Kit-8 (CCK-8) analysis. Our results showed that DHM has no obvious effect on HK-2 cell growth for 24 or 48 h at different concentrations (Figure S1B). As shown in Figure 6A, DHM could markedly inhibit TGF-β1-induced miR-34a upregulation in HK-2 cells. Moreover, DHM significantly attenuated the decreases in the expressions of Klotho and E-cadherin, and the increases in the expressions of α-SMA and fibronectin in TGF-β1-treated HK-2 cells (Figures 6B–6D). Previous studies reveal that miR-34a is the downstream target of p53, and TGF-β1 can regulate p53 activity in HK-2 cells.[35] p53 Ser^{15} phosphorylation is a form of p53 activation.[36,37] In our study, RNAi approach

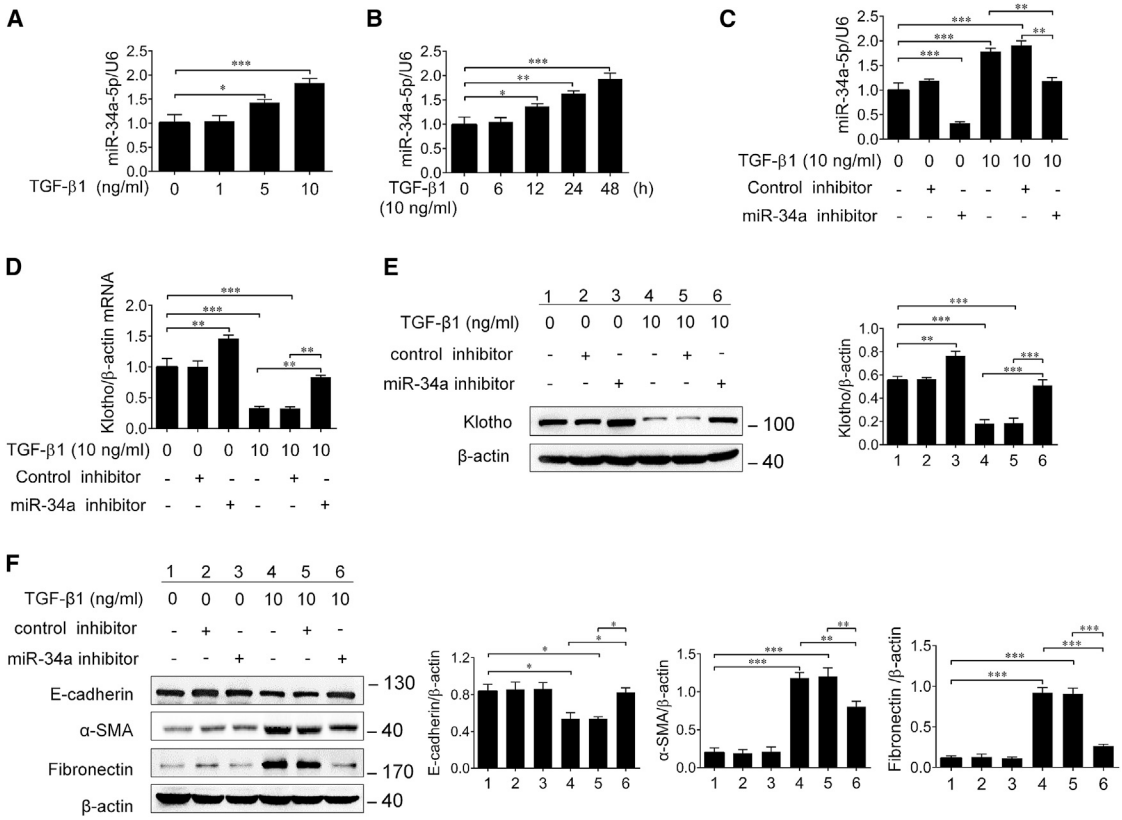

Figure 5. TGF-β1 Induced the Elevation of miR-34a and Downregulation of Klotho in HK-2 Cells

(A) qRT-PCR analysis of miR-34a expression in the HK-2 cells treated with different concentrations of TGF-β1 for 24 h. (B) qRT-PCR analysis of miR-34a expression in the HK-2 cells treated with 10 ng/mL TGF-β1 at different time. (C) qRT-PCR analysis of miR-34a expression in the HK-2 cells transfected with miR-34a inhibitor or control inhibitor. (D and E) qRT-PCR (D) and western blotting (E) analysis of Klotho in HK-2 cells after transfection with miR-34a inhibitor or control inhibitor followed by incubation with 10 ng/mL TGF-β1 for 48 h. (F) Western blotting analysis of E-cadherin, α-SMA, and fibronectin in HK-2 cells after transfection with miR-34a inhibitor or control inhibitor followed by incubation with 10 ng/mL TGF-β1 for 48 h. Data are means ± SD. ***$p < 0.001$, **$p < 0.01$, *$p < 0.05$.

was employed by p53 short hairpin RNA (shRNA) according to previous reports,[38,39] and the protein levels of p53 and phosphorylated p53 were simultaneously reduced by p53 shRNA in HK-2 cells. Notably, our results showed that TGF-β1-induced miR-34a upregulation in HK-2 cells was markedly relieved by transfection with p53 shRNA (Figures 6E and 6F). Furthermore, DHM could significantly inhibit p53 Ser^{15} phosphorylation induced by TGF-β1 (Figure 6G), whereas transfection with miR-34a mimic could evidently reverse the effects of DHM (Figures 6H–6J). These results demonstrate that DHM indeed has the ability to inhibit miR-34a upregulation in tubular epithelial cells, through suppressing TGF-β1-induced p53 phosphorylation.

DHM Inhibits the Progression of Renal Fibrosis in UUO Mice and ADR Nephropathy

Finally, to investigate the beneficial effect of DHM on renal fibrosis, UUO mice were intragastrically administered with DHM (500 mg/kg/day), starting from 7 days before surgery. As expected, DHM treatment significantly inhibited miR-34a elevation and rescued Klotho reduction in the obstructed kidney of UUO mice (Figures 7A–7E), accompanied by evident attenuation of the activations of pro-fibrotic signaling pathways (Figure 7F). Correspondingly, DHM administration resulted in an obvious attenuation of renal fibrosis in the obstructed kidney, as evaluated by H&E and Masson staining (Figures 8A and 8B). Meanwhile, the aberrant expressions of E-cadherin, α-SMA, and fibronectin and the increase of serum creatinine and blood urea nitrogen level were significantly reversed by DHM (Figures 8C–8E). We further investigated the therapeutic effects of DHM on Adriamycin (ADR) nephropathy, a model characterized by initial podocyte injury and albuminuria, and subsequent renal fibrosis. DHM and ADR (a single intravenous injection of ADR at 10 mg/kg body weight) were administered simultaneously and continued for 6 weeks in BALB/c mice. The different DHM administration time in UUO and ADR models attributed to their acute and chronic injury characteristics, and reference to previous studies.[40,41] Consistently, DHM attenuated renal fibrosis and kidney injury in ADR nephropathy, as evaluated by H&E and Masson staining (Figures 8F and 8G). In addition, DHM administration significantly attenuated ADR-induced albuminuria and the elevation of serum creatinine (Figure 8H). All of these findings suggest that

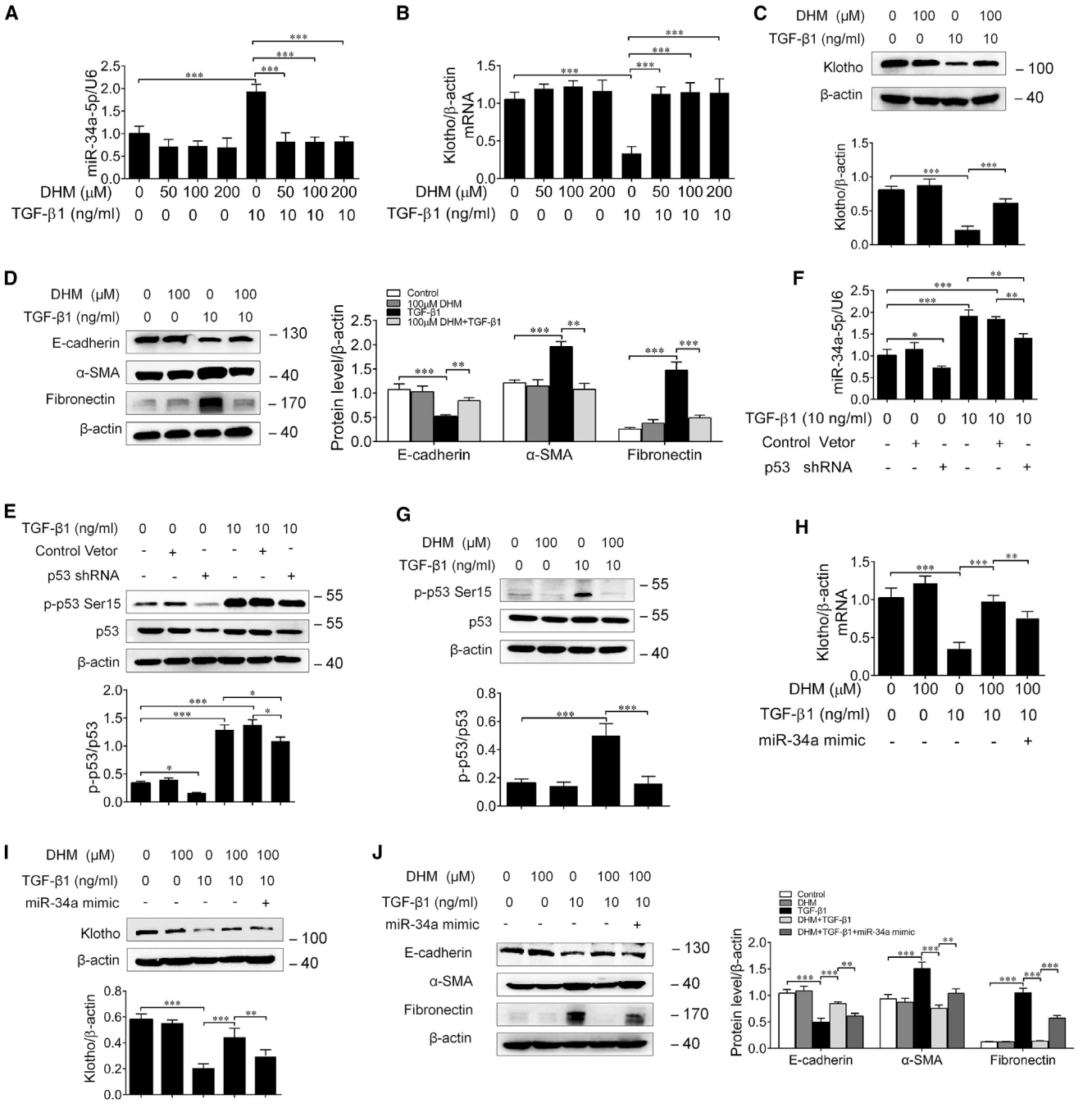

Figure 6. DHM Inhibited TGF-β1-Induced Upregulation of miR-34a and Retained Klotho Expression in HK-2 Cells

(A) qRT-PCR analysis of miR-34a expression in the HK-2 cells pretreated with different concentrations of DHM for 24 h followed by incubation with 10 ng/mL TGF-β1 for 24 or 48 h. (B) qRT-PCR analysis of Klotho in HK-2 cells pretreated with different concentrations of DHM for 24 h followed by incubation with 10 ng/mL TGF-β1 for 48 h. (C) Western blotting analysis of Klotho in HK-2 cells pretreated with DHM (100 μM) for 24 h followed by incubation with 10 ng/mL TGF-β1 for 48 h. (D) Western blotting analysis of E-cadherin, α-SMA, and fibronectin in HK-2 cells pretreated with of DHM (100 μM) for 24 h followed by incubation with 10 ng/mL TGF-β1 for 48 h. (E) Western blotting analysis for p-p53 Ser^{15} and p53 protein levels in HK-2 cells transfected with p53 shRNA or control-vector followed by incubation with 10 ng/mL TGF-β1 for 48 h. (F) qRT-PCR analysis of miR-34a expression in the HK-2 cells transfected with p53 shRNA or control-vector followed by incubation with 10 ng/mL TGF-β1 for 48 h. p53 shRNA significantly attenuated

(legend continued on next page)

DHM can protect against renal fibrosis through inhibiting miR-34a aberrant upregulation.

DISCUSSION

Huge studies have focused on the pathogenesis of renal fibrosis in recent years, but the molecular mechanisms underlying the progression of renal fibrosis are not fully understood, and there is still a lack of effective avenues for the clinical treatment of renal fibrosis. This is the pioneer study, in which we report that miR-34a contributes to renal fibrosis at least in part by downregulation of Klotho. Moreover, it is also shown that DHM, a natural flavonoid derived from the Chinese herb *Ampelopsis grossedentata*, can rescue miR-34a-mediated Klotho reduction in tubular epithelial cells and inhibit the progression of renal fibrosis in the ADR nephropathy and UUO model mice. Thus, current findings not only provide new insights into the molecular mechanism of renal fibrosis, but also find a new avenue for the treatment of renal fibrosis.

Previously, important roles of elevated miRs in certain kidney diseases were extensively reported and indicated that inhibition of these miRs might be a potential therapeutic target to cure these diseases. For example, miR-92a was reported to be upregulated in podocytes of both patients and mice with rapidly progressive glomerulonephritis (RPGN), whereas anti-miR-92a treatment could prevent albuminuria and the decline of kidney function.[42] Another study showed that upregulation of miR-184 in renal tubular was associated with decreased expression of lipid phosphate phosphatase 3 (LPP3) and collagen accumulation in Zucker diabetic fatty (ZDF) rats, and angiotensin-converting enzyme (ACE) inhibitor treatment could preserve LPP3 and ameliorate tubule interstitial fibrosis through suppressing miR-184.[43] Furthermore, our study also showed that miR-34a was significantly upregulated in kidney tubules in UUO mice. The *in vitro* experiments demonstrated that transfection of cultured proximal tubular cells with miR-34a mimic could increase α-SMA and fibronectin expression, while decreasing the E-cadherin expression. On the contrary, by using miR-34a$^{-/-}$ mice, we found miR-34 deficiency could alleviate renal fibrosis after obstructive injury. These results simply demonstrated that elevated miR-34a may play an important role in the progression of renal fibrosis. Previous studies have revealed that miR-34a contributed to renal fibrosis under diabetic conditions by suppressing SIRT1[44,45] and induced tubular cell apoptosis in the obstructed kidney.[46] Thus, our results were consistent with these previous studies, but our study, by using miR-34a knockout mice, was more convincing in proving the role of miR-34a in promoting renal fibrosis.

Next the results showed that miR-34a promoted the progression of renal fibrosis at least in part through downregulation of the *Klotho* gene. Klotho, which is predominately expressed in renal tubular epithelial cells and initially known as an anti-aging gene,[47] has been reported to play a crucial role in protecting the kidneys against acute and chronic injury.[29,48,49] Previous studies, including the results of the current study, revealed that renal Klotho is markedly downregulated in tubular epithelial cells in patients or experimental animal models with kidney diseases.[50–52] As demonstrated, Klotho reduction may accelerate pro-fibrotic phenotype transition in tubular epithelial cells and enhances the proliferation of fibroblasts, whereas Klotho overexpression or exogenous supplement can alleviate renal fibrosis by suppressing pro-fibrotic signaling pathways, including TGF-β1, Wnt, and FGF2 pathways.[29,48,49] In this study, we found that miR-34a mimic significantly reduced Klotho expression in cultured proximal tubular cells and then revealed that miR-34a downregulated Klotho by directly binding to the 3′ UTR of *Klotho* mRNA. On the other hand, it was disclosed that miR-34a$^{-/-}$ UUO mice displayed an attenuated Klotho reduction and renal fibrosis. All these findings suggest that Klotho is a downstream target of miR-34a, and the upregulated miR-34a in obstructed kidney may cause Klotho reduction, which leads to enhanced activation of pro-fibrotic signaling pathways and promotion of the progression of renal fibrosis. Of note, although the Klotho expression level in miR-34a$^{-/-}$ mice was four to five times higher than that of the WT UUO mice, the expression level of Klotho was still much lower than that in control mice. This indicates that the aberrant elevation of miR-34a is not the sole regulatory factor for reduction of Klotho. Therefore, further research is required to illustrate other regulatory mechanisms. Nevertheless, because Klotho is a strong inhibitor of several classical pro-fibrogenic signaling pathways, upregulation of Klotho through suppressing miR-34a level in tubular epithelial cells could still be considered as an important therapeutic target for renal fibrosis.

It is well-known that TGF-β1 is a pivotal mediator in the pathogenesis of renal fibrosis. A number of studies reported that TGF-β1 exerted its functions partly through the regulation of certain miRs, including upregulation of miR-192, miR-377, and miR-491, but downregulation of miR-29 and miR-30, in mesangial cells and podocytes.[16,17,30–32] Herein, it was also found that TGF-β1 induced a significant upregulation of miR-34a in cultured proximal tubular cells in a dose- and time-dependant manner, and miR-34a inhibitor could markedly reverse TGF-β1-induced tubular epithelial cells plasticity. Therefore, our study also demonstrates that TGF-β1 has the ability to increase miR-34a expression. Moreover, a significant reduction of Klotho was observed in TGF-β1-treated tubular cells, possibly because of the upregulation of miR-34a. Because the reduction of Klotho in tubular epithelial cells can enhance TGF-β1 signaling activation,[48] the findings of the present study indicate that miR-34a upregulation may mediate a feedback loop between TGF-β1 activation and Klotho reduction in the progression of renal fibrosis (Figure 8H).

TGF-β1-induced elevated miR-34a expression. (G) Western blotting analysis for p-p53 Ser^{15} and p53 protein levels in HK-2 cells pretreated with DHM for 24 h followed by incubation with 10 ng/mL TGF-β1 for 48 h. (H and I) qRT-PCR (H) and western blotting (I) analysis of Klotho in HK-2 cells pretreated with DHM for 24 h followed by incubation with 10 ng/mL TGF-β1 for 48 h or transfected with miR-34a mimic. (J) Western blotting analysis of E-cadherin, α-SMA, and fibronectin in HK-2 cells pretreated with DHM for 24 h followed by incubation with 10 ng/mL TGF-β1 for 48 h or transfected with miR-34a mimic. Data are means ± SD. ***$p < 0.001$, **$p < 0.01$, *$p < 0.05$.

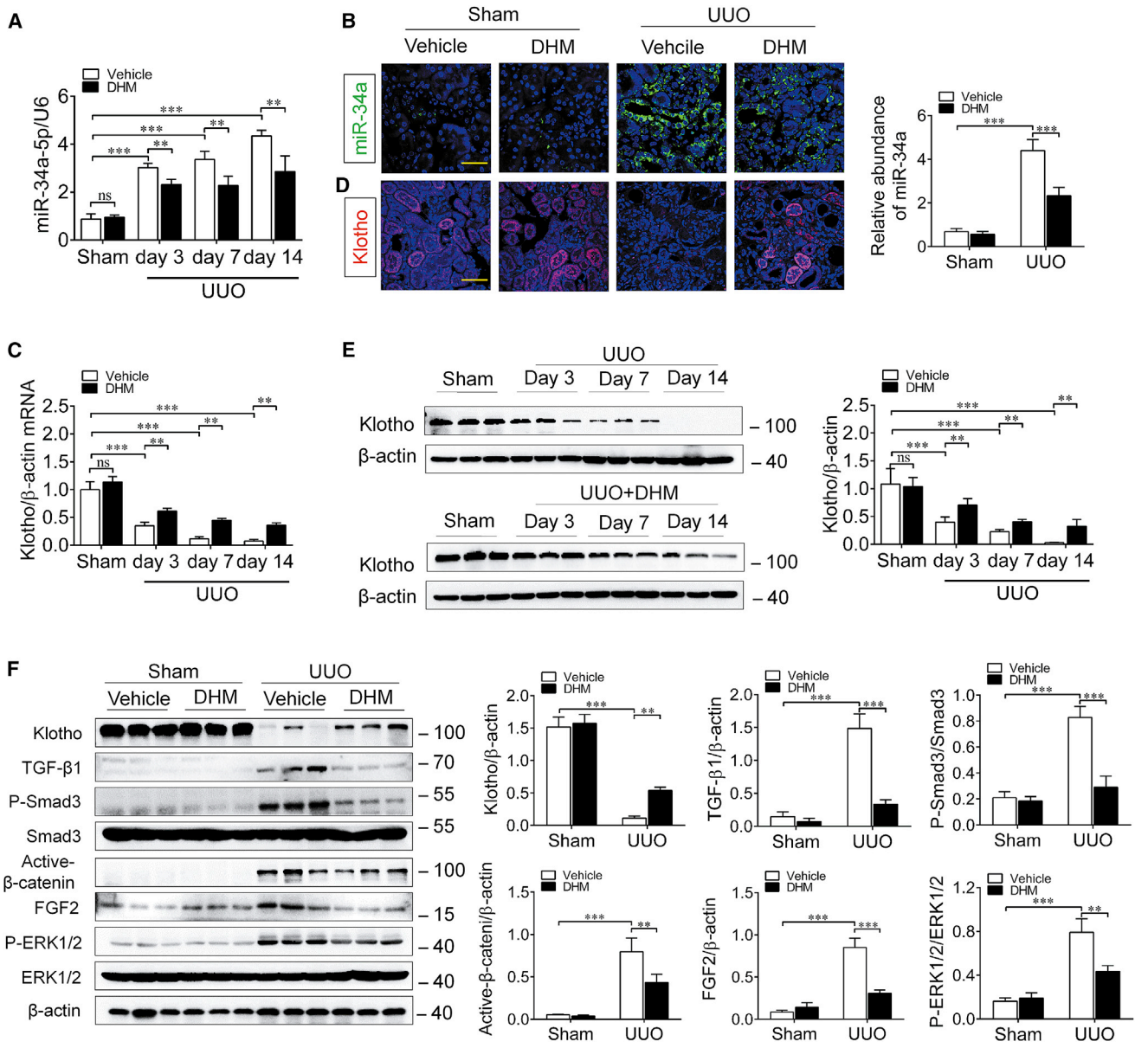

Figure 7. DHM Inhibited the Elevation of miR-34a and Klotho Deficiency in UUO Mice

(A) qRT-PCR analysis of the expression level of miR-34a in the mouse obstructed kidney at 3, 7, and 14 days after UUO surgery. U6 was used for normalization. (B) Representative images showing the expression and localization of miR-34a at 14 days after UUO by *in situ* hybridization. Quantification of miR-34a in the mouse obstructed kidney at 14 days after UUO surgery. miR-34a (green) and DAPI (blue). The scale bar corresponds to 50 μm. (C) qRT-PCR analysis of Klotho mRNA expression in the mouse obstructed kidney at 14 days after UUO surgery. (D) Representative immunofluorescence of Klotho in the mouse obstructed kidneys at 14 days after UUO surgery. Klotho (red) and DAPI (blue). The scale bar corresponds to 50 μm. (E) Western blotting analysis for Klotho in the mouse obstructed kidney at 3, 7, and 14 days after UUO surgery. (F) Western blotting analysis for Klotho, TGF-β1, phospho-smad3, active-β-catenin, FGF2, and phospho-ERK1/2 protein levels in UUO mice at 14 days after surgery. Data are means ± SD. n = 6 mice per group. ***p < 0.001, **p < 0.01, *p < 0.05.

DHM enriched in *Ampelopsis grossedentata* is being used as a traditional Chinese herb throughout China due to its hepatoprotective effects.[23] Recently, DHM was found to have protective effects against AKI, because it could markedly attenuate cisplatin-induced apoptosis of renal tubular epithelial cells and ameliorate the impairment of renal function induced by lipopolysaccharides.[53,54] As reported, miR-34a upregulation was involved in certain diseases that are associated with oxidative stress, inflammation, and aging, by downregulating sirtuin-1, sirtuin-6, SOD2, and Txnrd2.[55,56] Notably, it has been demonstrated that DHM not only has significant anti-oxidation activities,

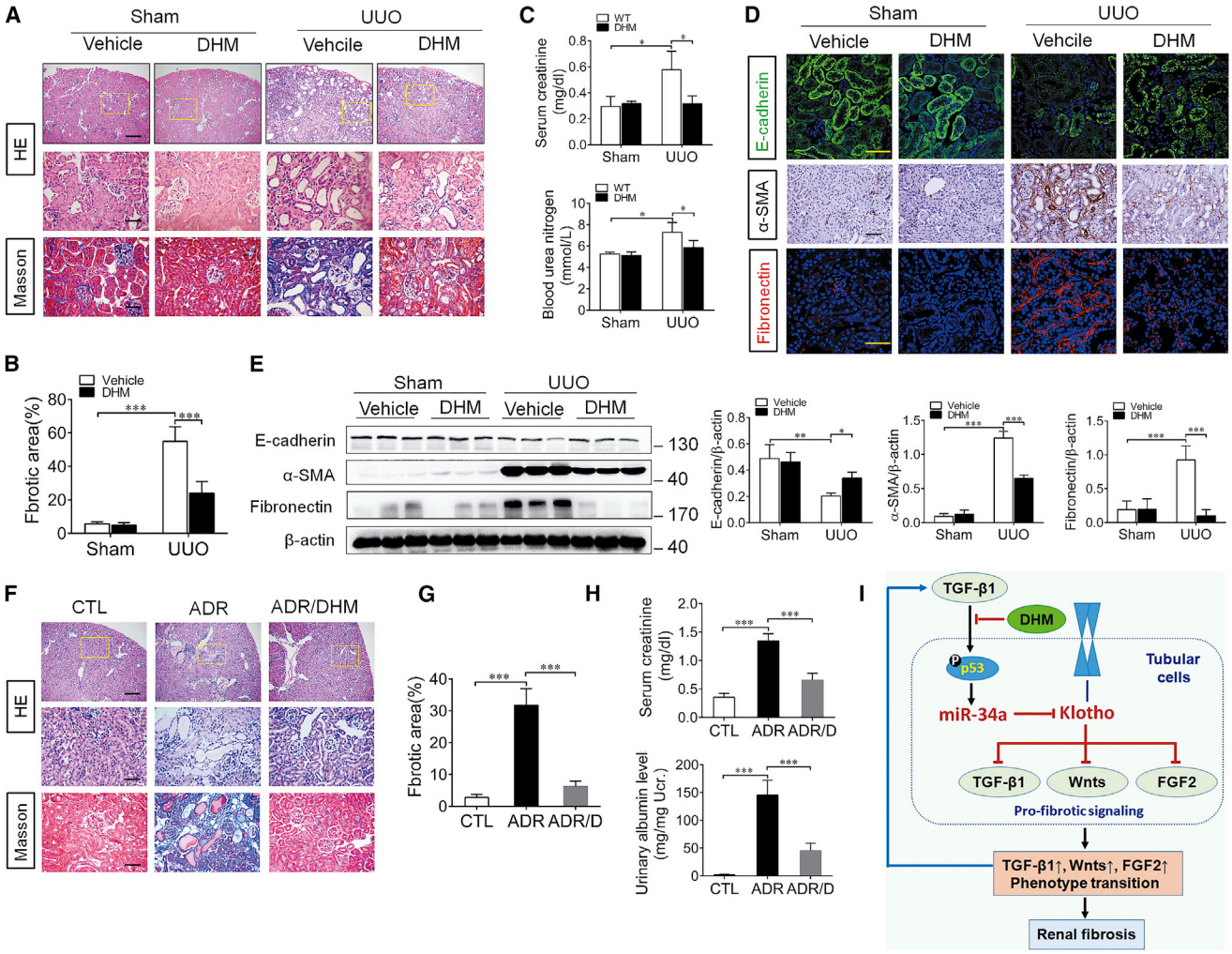

Figure 8. DHM Attenuated Renal Fibrosis and Kidney Injury in UUO Mice and Adriamycin Nephropathy

(A) Representative micrographs of H&E and Masson trichrome staining of mouse kidney sections at 14 days after UUO surgery. The fibrotic lesions were indicated by blue color areas in the center. The top scale bar corresponds to 200 μm; the center and bottom scale bars correspond to 50 μm. (B) Graphical presentation of kidney fibrotic lesions in different groups after quantitative determination. (C) Serum creatinine and blood urea nitrogen were assessed at 14 days after UUO surgery. (D) Representative immunostaining of E-cadherin, α-SMA, and fibronectin in the obstructed kidneys at 14 days after UUO surgery. E-cadherin (green), fibronectin (red), and DAPI (blue) are shown. The scale bars correspond to 50 μm. (E) Western blotting analysis for E-cadherin, α-SMA, and fibronectin protein levels in UUO mice at 14 days after surgery. (F) Representative micrographs of H&E and Masson trichrome staining of mouse kidney sections at 5 weeks days after ADR injection in different groups of mice as indicated. The fibrotic lesions were indicated by blue color areas in the center. The top scale bar corresponds to 200 μm; the center and bottom scale bars correspond to 50 μm. (G) Graphical presentation of kidney fibrotic lesions in different groups after quantitative determination. (H) Serum creatinine and urinary albumin were assessed at 5 weeks after ADR injection. Urinary albumin levels expressed as milligram per milligram (mg/mg) creatinine in different groups of mice. DHM reduced serum creatinine levels and urinary albumin in Adriamycin nephropathy. (I) Schematic illustration of the role of miR-34a in regulating renal fibrosis. TGF-β1 induces an aberrant miR-34a expression in renal tubular epithelial cells through p53 activation. miR-34a promotes renal fibrosis by downregulation of Klotho, which alleviates renal fibrosis by suppressing pro-fibrotic signaling pathways, including TGF-β1, Wnt, and FGF2 pathways. DHM may reverse the upregulation of miR-34a and Klotho reduction by inhibition of TGF-β1-induced p53 activation. In addition, the elevated expression of miR-34a may mediate a vicious cycle of sustained progression of renal fibrosis. Data are means ± SD. n = 6 mice per group. ***p < 0.001, **p < 0.01, *p < 0.05. ADR, Adriamycin; CTL, control; DHM, dihydromyricetin.

but also possesses an inhibitory effect against the action of miR-34a.[34] The current study found that DHM could significantly repress the up-regulation of miR-34a induced by TGF-β1 and restore Klotho expression, thereby inhibiting the progression of renal fibrosis. As known, miR-34a is the downstream target of p53.[57] p53 could significantly induce the transcription of miR-34a because p53 occupies a highly conserved consensus binding site that is located in close proximity to the transcription start site of miR-34a.[57–59] Recent studies show that TGF-β1-stimulated activation of p53 is required for expression of the fibrotic genes and renal fibrosis.[35] Pharmacological and genetic blockade of p53 prevented tubular cell-cycle arrest, fibrotic factor secretion, apoptosis, and renal interstitial fibrosis in UUO mice.[60,61]

It was further confirmed in the present study that DHM inhibits the expression of miR-34a in tubular epithelial cells because of its inhibition of TGF-β1-stimulated p53 activation. Moreover, DHM also ameliorates renal fibrosis and kidney injury in ADR nephropathy, suggesting that DHM attenuated renal fibrosis is a common finding in diseased kidneys after various injuries. Furthermore, we think that DHM has a potential and good advantage to be used for the treatment of human diseases. First, medicinal tea (vine tea), a natural product, and DHM are the most prominent flavonoids in vine tea. Second, DHM exerts many biologic effects and has no side effects and cytotoxicity. Third, a randomized controlled trial has reported that DHM improves glucose and lipid metabolism, and exerts anti-inflammatory effects in patients with nonalcoholic fatty liver disease.[62] In our study, DHM administration dramatically ameliorated renal fibrosis and restored renal function in an ADR nephropathy and UUO model mice. Collectively, our findings provide evidence that DHM has the potential to be used for the treatment of renal fibrosis in clinic.

In summary, the results herein demonstrate that aberrant upregulation of miR-34a plays an important role in the progression of renal fibrosis, and DHM has the potential to treat renal fibrosis by the inhibition of miR-34a. These findings may shed new light on the pathogenesis and treatment of renal fibrosis.

MATERIALS AND METHODS

Animal Experiments

The mice were randomly assigned to either UUO (n = 6) or sham (n = 6) groups. Eight-week-old male C57BL/6 mice and miR-34a knockout (miR-34a$^{-/-}$) mice (obtained from The Jackson Laboratory) weighing 20–23 g were anaesthetized with an intraperitoneal injection of pentobarbital. The UUO mice were subjected to a left lateral incision, and the left ureter was double-ligated with 4–0 silk. Sham groups underwent only the surgical procedure of kidney exposure, but not ligation. miR-34a$^{-/-}$ mice and WT (miR-34a$^{+/+}$) mice were sacrificed 14 days after surgery (for each group, n = 5). In another set of experiments with DHM, the mice were divided into four groups: Sham+Vehicle (injection with 0.9% saline), Sham+DHM, UUO+Vehicle, and UUO+DHM. DHM (500 mg/kg/day) (MCE, USA) was suspended in 0.9% saline and intragastrically administered to C57BL/6J mice 7 days ago before UUO surgery and continued to the end of the experiment. The mice were sacrificed at 3, 7, and 14 days (for each group, n = 6), and the obstructed kidneys were collected for various analyses. All animal studies were performed according to the guiding principles established by the Institutional Animal Care and Use Committee (IACUC) of the Third Military Medical University.

For studying the effects of DHM on ADR nephropathy, male BALB/C mice weighing 20–25 g were randomly divided into three groups: (1) control (CTL) group (n = 5); (2) ADR group (n = 9), and (3) ADR/DHM group (n = 9). ADR (doxorubicin hydrochloride; MCE, USA) was injected once via the tail vein at 10 mg/kg body weight. Control mice were injected with the same volume of saline. For the ADR/DHM group, DHM was given by daily intragastrically administration at 500 mg/kg body weight, starting at the time when ADR was administered. All mice were sacrificed at 5 weeks after ADR injection.

Selection of CKD Patients

Eight primary CKD patients with renal fibrosis (glomerular filtration rate [eGFR]: 10.92–58.52 mL/min/1.73 m^2) verified by renal biopsy were enrolled from Department of Nephrology of Xinqiao Hospital (Chongqing, China). Five patients with eGFR >110 mL/min/1.73 m^2 and almost nonlesions verified by renal biopsy were enrolled as control. The following exclusion criteria were applied: polycystic kidney disease, pregnancy, HIV, renal cancer, and recent immunosuppressive therapy. Kidney biopsies were obtained from these patients for subsequent Masson trichrome staining and *in situ* hybridization. The study protocol was approved by the Ethics Committee of Xinqiao Hospital and carried out in accordance with the Declaration of Helsinki.

Cell Culture and Treatment

Human proximal tubular cells (HK-2 cells) were purchased from the American Tissue Culture Collection (ATCC, Manassas, VA, USA) and cultured in DMEM/F12 medium supplemented with 10% fetal bovine serum (GIBCO BRL, Rockville, MD, USA) at 37°C in a humidified atmosphere with 5% CO_2. After being seeded into six-well plates for 24 h, HK-2 cells were replaced with normal media in the absence or presence of DHM (50, 100, or 200 μm) for 24 or 48 h. To further determine the effects of DHM on HK-2 cells, we pre-incubated cells with DHM for 24 h and subsequently exposed them to TGF-β1 (10 ng/mL) for 24 or 48 h.

qRT-PCR

Total RNA was extracted from the mouse kidney and HK-2 cells using TRIzol Reagent Kit (Invitrogen, Carlsbad, CA, USA). For miR-34a, total RNA (2 μg) was reverse transcribed into cDNA using a microRNA First-Strand cDNA Synthesis Kit (Sangong Biotech, Shanghai, China) according to the manufacturer's protocol. The specific forward primer for mmu-miR-34a was 5′-TGGCAGTGTCT TAGCTGGTT-3′. The specific forward primer for has-miR-34a is 5′-CGAATCAGCAAGTATACTGCCCT-3′. To relatively quantify the miR-34a expression levels, we used small nuclear U6 as the internal control. For mRNA expression analysis, cDNAs were obtained by the GoScript Reverse Transcription System Kit (Promega, Madison, WI, USA). The specific primer for mmu-Klotho was 5′-AAAGTAG ACGGGGTTGTAGCC-3′, 5′-CGGTAGAAGTGCAGAACCGT-3′. The specific primer for has-Klotho was 5′-TAGCCAGCGACAGC TACAAC-3′, 5′-GAAGCGGTAGTGAGTGACCC-3′. miRNA and mRNA expression were examined using a Bio-Rad IQ5 Detection System with SYBR Green PCR Master mix (Promega, USA) as previously described.

Fluorescence *In Situ* Hybridization

In situ hybridization was performed with probes for human or mouse miR-34a (38487-15; ExiQon, Denmark) and control sequences according to the manufacturer's protocol. In brief, sections of paraffin-embedded specimens from CKD patients with renal fibrosis

and mouse kidney tissue were deparaffinized and rehydrated. After being washed with PBS, sections were incubated with 20 μg/mL Proteinase K for 10 min at 25°C, followed by incubation with 1-(3-dimethylaminopropyl)-3-ethylcarbodiimide hydrochloride (EDC) fixation solution for 30 min. Then slides were hybridized with a 5′-digoxigenin (DIG)-labeled oligonucleotide probe complementary (50 nM) to miR-34a or a control probe (Perkin Elmer) at 60°C for 2 h. Sections were washed in washing buffer I (5× saline sodium citrate [SSC], 60°C), washing buffer II (1× SSC), and washing buffer III (0.2× SSC), and then were incubated with blocking reagent at room temperature for 30 min. Sections were then stained with anti-digoxigenin-peroxidase (POD) (11207-733910; Roche, USA) for 1.5 h. After being washed with Tris and Nacl (TNT) buffer, sections were incubated with TSA Plus Fluorescein kit (NEL744001-KT; Perkin Elmer) away from light. Sections were then mounted with antifade mounting medium by using DAPI to visualize the nuclei (Invitrogen Molecular Probes, Eugene, OR, USA). For double-immunofluorescence staining with *in situ* hybridization and immunofluorescence, slides were then incubated with Klotho (ab203576; Abcam) overnight at 4°C after *in situ* hybridization. Slides were visualized on a ZEISS confocal microscope. Fluorescence quantitation of miR-34a was analyzed by Image-Pro Plus software.

Cell Transfection

miR-34a mimic, inhibitor, and their negative controls were purchased from RiboBio (RiboBio, Guangzhou, China). For overexpression of Klotho, pReceiver-Lv105 Klotho open reading frame (ORF) lentiviral expression clone and vector were purchased from Genecopoeia (Rockville, MD, USA). p53 shRNA construct and control vector were obtained from Genechem (Shanghai, China). HK-2 cells were cultured in a 12- or 6-well plate 24 h before transfection. Prior to miRNA transfection, the cell culture medium of the HK-2 cells was replaced with serum-reduced medium (Opti-MEM I; Invitrogen, Carlsbad, CA, USA). The transfection was performed with Lipofectamine 2000 (Invitrogen) according to the manufacturer's instructions. For Klotho and miR-34a mimic cotransfection, the plasmid (4 μg) and miR-34a mimic that was prepared with lipid carrier (1:2, v/v) was used for the transfection in Opti-MEM I medium. HK-2 cells were incubated with the mimic or inhibitor (100 nM)/Lipofectamine mixture for 6 h. Then the Opti-MEM I medium was switched to a growth medium. To determine the optimal transfection conditions, we confirmed the transfection efficiency by real-time PCR.

Western Blotting

Proteins isolated from kidney tissue samples and cultured HK-2 cells were separated by SDS-PAGE and transferred to polyvinylidene fluoride (PVDF) membranes (Millipore, Billerica, MA, USA), blocked with 5% non-fat dried milk, and incubated at 4°C overnight with primary antibodies: anti-E-cadherin antibody (20874-1-AP; Proteintech, USA), anti-α-SMA antibody (ab5694; Abcam, Cambridge, MA, USA), anti-fibronectin antibody (15613-1-AP; Proteintech, USA), anti-Klotho antibody (ab203576; Abcam), anti-p53 antibody (9282; Cell Signaling Technology, Beverly, MA, USA), anti-phosphorylation-p53 Ser^{15} antibody (ab1431; Abcam), anti-phospho-p44/42 mitogen-activated protein kinase (MAPK) (ERK1/2) (Thr202/Tyr204) (4370; CST), anti-total ERK1/2 (4696; CST), anti-phospho-Smad3 (Ser423/425) (9520; CST), anti-total Smad3 (9513; CST), and anti-β-actin antibody (4970; CST). Then the secondary antibodies were applied and the signals were detected by enhanced chemiluminescence (Amersham Corporation, Arlington Heights, IL, USA). The density of the bands was quantified using ImageJ software and normalized against that of β-actin.

Luciferase Reporter Assay

The human Klotho fragments containing putative binding sites located in the 3′ UTR were amplified by PCR by using human genomic DNA as a template. The PCR products were inserted into the p-MIR-REPORT plasmid (Invitrogen) and confirmed by sequencing. The specific primer for human 3′ UTR-*Klotho* is 5′-GCC GAGCTCATGGGCATAGGTGATCGTAA-3′, 5′-CGCAA GCTT TCCACAGAAGTAGCAGCAAA-3′. To test the binding specificity, the putative binding sites of miR-34a in the human Klotho 3′ UTR were mutated by PCR (human, from 5′-CUGCCA-3′ to 5′-AUGACA-3′). For the luciferase reporter assay, HK-2 cells were cultured in 24-well plates and transfected each well with 500 ng of firefly luciferase reporter plasmid cotransfected with miR-34a mimic at different concentration or negative control RNA by using Lipofectamine 2000. An internal control reporter plasmid (10 ng) Renilla reniformis luciferase (Promega, Madison, WI, USA) was also co-transfected for normalizing the transfection efficiency. Luciferase activities were measured at 24 h after transfection using dual-luciferase assay kits according to the manufacturer's protocols (Promega). Relative luciferase activity (arbitrary units) was reported as fold induction over the controls after normalizing for transfection efficiency.

Histology and Immunohistochemical Staining

Paraffin-embedded mouse kidney sections were prepared by a routine procedure. Sections were stained with H&E and Masson trichrome staining to detect interstitial volume expansion (blue staining). Quantification of the fibrotic area was carried out by using Image Pro-Plus v. 6.0 software (Bethesda, MD, USA). Immunostaining for α-SMA was performed as described previously.[29] The kidney sections were incubated with the primary antibodies (1:100, ab5694; Abcam, Cambridge, MA, USA) overnight at 4°C, followed by incubation with the biotinylated-linked secondary antibodies for 1 h at 37°C and developed with 3,3′-diaminobenzidine (DAB). The tissue sections were counterstained with hematoxylin and permanently mounted. As a negative control, PBS was used instead of a primary antibody.

Immunofluorescence Assay

The paraffin-embedded mouse kidney sections were prepared by a routine procedure and then incubated with anti-E-cadherin antibody (1:200, 20874-1-AP; Proteintech, USA), anti-fibronectin antibody (1:200, 15613-1-AP; Proteintech, USA), or Klotho (ab203576; Abcam) overnight at 4°C. The slides were then stained by Cy3- or fluorescein isothiocyanate (FITC)-conjugated secondary antibody for 1 h at 37°C and mounted with antifade mounting medium by using

DAPI to visualize the nuclei. Slides were visualized on a ZEISS confocal microscope.

Urinary Albumin and Creatinine Assay

Urine albumin was measured by using a mouse albumin ELISA quantitation kit, according to the manufacturer's protocol (Bethyl Laboratories, Montgomery, TX, USA). Serum creatinine level and urine creatinine were determined by use of a Quantichrom creatinine assay kit (C011-2; njjcbio, China), according to the protocols specified by the manufacturer. Urinary albumin was standardized to urine creatinine and expressed as milligram per milligram (mg/mg) urinary creatinine. Serum creatinine level was determined by use of a Quantichrom creatinine assay kit (DICT-500; Bioassay Systems, Hayward, CA, USA), according to the protocols specified by the manufacturer.

Statistical Analysis

All results were expressed as the mean ± SD. Statistical analysis was performed with GraphPad Prism 6.0 (San Diego, CA, USA). A t test was used to test the differences between two groups, and comparisons among multiple groups were performed with a one-way ANOVA followed by Tukey's post hoc test. A p value <0.05 was considered to be statistically significant. All data were obtained from at least three independent experiments.

SUPPLEMENTAL INFORMATION

Supplemental Information includes Supplemental Materials and Methods, one figure, and one table and can be found with this article online at https://doi.org/10.1016/j.ymthe.2019.02.009.

AUTHOR CONTRIBUTIONS

Y. Liu and X.B. performed experiments, analyzed data, and wrote the paper. J.X., W.H., and W.J. contributed to construction of plasmids. X.X., T.X., and Y. Li contributed to animal experiments and data analysis. T.H., C.L., K.Y., Y.Y., Y. Li, and J.Z. contributed to the *in vitro* experiments. B.Z. and J.Z. contributed to the initial experimental design and discussed the manuscript. J.Z. conceived and supervised the study, analyzed the data, and wrote and revised the manuscript.

CONFLICTS OF INTEREST

The authors declare no competing interests.

ACKNOWLEDGMENTS

This study was supported by research grants from the National Key Technology Research and Development Program of China (2017YFA0106600), the National Natural Science Foundation of China (81873605, 81800621, 81700379, 81800616, 81800640, and 81600569), Personnel Training Program for Clinical Medicine Research of Army Medical University (2018XLC1007), and Frontier specific projects of Xinqiao Hospital (2018YQYLY004).

REFERENCES

1. Coresh, J., Selvin, E., Stevens, L.A., Manzi, J., Kusek, J.W., Eggers, P., Van Lente, F., and Levey, A.S. (2007). Prevalence of chronic kidney disease in the United States. JAMA *298*, 2038–2047.

2. Cheikh Hassan, H.I., Tang, M., Djurdjev, O., Langsford, D., Sood, M.M., and Levin, A. (2016). Infection in advanced chronic kidney disease leads to increased risk of cardiovascular events, end-stage kidney disease and mortality. Kidney Int. *90*, 897–904.

3. McClellan, A.C., Plantinga, L., and McClellan, W.M. (2012). Epidemiology, geography and chronic kidney disease. Curr. Opin. Nephrol. Hypertens. *21*, 323–328.

4. Drey, N., Roderick, P., Mullee, M., and Rogerson, M. (2003). A population-based study of the incidence and outcomes of diagnosed chronic kidney disease. Am. J. Kidney Dis. *42*, 677–684.

5. Tampe, D., and Zeisberg, M. (2014). Potential approaches to reverse or repair renal fibrosis. Nat. Rev. Nephrol. *10*, 226–237.

6. Neilson, E.G. (2006). Mechanisms of disease: fibroblasts—a new look at an old problem. Nat. Clin. Pract. Nephrol. *2*, 101–108.

7. Strutz, F., and Zeisberg, M. (2006). Renal fibroblasts and myofibroblasts in chronic kidney disease. J. Am. Soc. Nephrol. *17*, 2992–2998.

8. Liu, Y. (2010). New insights into epithelial-mesenchymal transition in kidney fibrosis. J. Am. Soc. Nephrol. *21*, 212–222.

9. Lovisa, S., LeBleu, V.S., Tampe, B., Sugimoto, H., Vadnagara, K., Carstens, J.L., Wu, C.C., Hagos, Y., Burckhardt, B.C., Pentcheva-Hoang, T., et al. (2015). Epithelial-to-mesenchymal transition induces cell cycle arrest and parenchymal damage in renal fibrosis. Nat. Med. *21*, 998–1009.

10. Zhang, B., Nguyen, L.X.T., Li, L., Zhao, D., Kumar, B., Wu, H., Lin, A., Pellicano, F., Hopcroft, L., Su, Y.L., et al. (2018). Bone marrow niche trafficking of miR-126 controls the self-renewal of leukemia stem cells in chronic myelogenous leukemia. Nat. Med. *24*, 450–462.

11. Song, C., Xu, Z., Jin, Y., Zhu, M., Wang, K., and Wang, N. (2015). The network of microRNAs, transcription factors, target genes and host genes in human renal cell carcinoma. Oncol. Lett. *9*, 498–506.

12. Zhao, Y., Ransom, J.F., Li, A., Vedantham, V., von Drehle, M., Muth, A.N., Tsuchihashi, T., McManus, M.T., Schwartz, R.J., and Srivastava, D. (2007). Dysregulation of cardiogenesis, cardiac conduction, and cell cycle in mice lacking miRNA-1-2. Cell *129*, 303–317.

13. van Rooij, E., Sutherland, L.B., Qi, X., Richardson, J.A., Hill, J., and Olson, E.N. (2007). Control of stress-dependent cardiac growth and gene expression by a microRNA. Science *316*, 575–579.

14. Yang, F., Chen, Q., He, S., Yang, M., Maguire, E.M., An, W., Afzal, T.A., Luong, L.A., Zhang, L., and Xiao, Q. (2018). miR-22 is a novel mediator of vascular smooth muscle cell phenotypic modulation and neointima formation. Circulation *137*, 1824–1841.

15. Chen, L.J., Chuang, L., Huang, Y.H., Zhou, J., Lim, S.H., Lee, C.I., Lin, W.W., Lin, T.E., Wang, W.L., Chen, L., et al. (2015). MicroRNA mediation of endothelial inflammatory response to smooth muscle cells and its inhibition by atheroprotective shear stress. Circ. Res. *116*, 1157–1169.

16. Esau, C., Davis, S., Murray, S.F., Yu, X.X., Pandey, S.K., Pear, M., Watts, L., Booten, S.L., Graham, M., McKay, R., et al. (2006). miR-122 regulation of lipid metabolism revealed by in vivo antisense targeting. Cell Metab. *3*, 87–98.

17. Calin, G.A., Sevignani, C., Dumitru, C.D., Hyslop, T., Noch, E., Yendamuri, S., Shimizu, M., Rattan, S., Bullrich, F., Negrini, M., and Croce, C.M. (2004). Human microRNA genes are frequently located at fragile sites and genomic regions involved in cancers. Proc. Natl. Acad. Sci. USA *101*, 2999–3004.

18. Nakagawa, N., Xin, C., Roach, A.M., Naiman, N., Shankland, S.J., Ligresti, G., Ren, S., Szak, S., Gomez, I.G., and Duffield, J.S. (2015). Dicer1 activity in the stromal compartment regulates nephron differentiation and vascular patterning during mammalian kidney organogenesis. Kidney Int. *87*, 1125–1140.

19. Wang, Q., Wang, Y., Minto, A.W., Wang, J., Shi, Q., Li, X., and Quigg, R.J. (2008). MicroRNA-377 is up-regulated and can lead to increased fibronectin production in diabetic nephropathy. FASEB J. *22*, 4126–4135.

20. Lorenzen, J.M., Kaucsar, T., Schauerte, C., Schmitt, R., Rong, S., Hübner, A., Scherf, K., Fiedler, J., Martino, F., Kumarswamy, R., et al. (2014). MicroRNA-24 antagonism prevents renal ischemia reperfusion injury. J. Am. Soc. Nephrol. *25*, 2717–2729.

21. Slabáková, E., Culig, Z., Remšík, J., and Souček, K. (2017). Alternative mechanisms of miR-34a regulation in cancer. Cell Death Dis. *8*, e3100.

22. Zhang, Y., Tao, X., Yin, L., Xu, L., Xu, Y., Qi, Y., Han, X., Song, S., Zhao, Y., Lin, Y., et al. (2017). Protective effects of dioscin against cisplatin-induced nephrotoxicity via the microRNA-34a/sirtuin 1 signalling pathway. Br. J. Pharmacol. *174*, 2512–2527.

23. Ye, L., Wang, H., Duncan, S.E., Eigel, W.N., and O'Keefe, S.F. (2015). Antioxidant activities of Vine Tea (Ampelopsis grossedentata) extract and its major component dihydromyricetin in soybean oil and cooked ground beef. Food Chem. *172*, 416–422.

24. Wu, B., Lin, J., Luo, J., Han, D., Fan, M., Guo, T., Tao, L., Yuan, M., and Yi, F. (2017). Dihydromyricetin protects against diabetic cardiomyopathy in streptozotocin-induced diabetic mice. BioMed Res. Int. *2017*, 3764370.

25. Le, L., Jiang, B., Wan, W., Zhai, W., Xu, L., Hu, K., and Xiao, P. (2016). Metabolomics reveals the protective of Dihydromyricetin on glucose homeostasis by enhancing insulin sensitivity. Sci. Rep. *6*, 36184.

26. Zhou, D.Z., Sun, H.Y., Yue, J.Q., Peng, Y., Chen, Y.M., and Zhong, Z.J. (2017). Dihydromyricetin induces apoptosis and cytoprotective autophagy through ROS-NF-κB signalling in human melanoma cells. Free Radic. Res. *51*, 517–528.

27. Lv, W., Booz, G.W., Wang, Y., Fan, F., and Roman, R.J. (2018). Inflammation and renal fibrosis: recent developments on key signaling molecules as potential therapeutic targets. Eur. J. Pharmacol. *820*, 65–76.

28. Kim, J., Seok, Y.M., Jung, K.J., and Park, K.M. (2009). Reactive oxygen species/oxidative stress contributes to progression of kidney fibrosis following transient ischemic injury in mice. Am. J. Physiol. Renal Physiol. *297*, F461–F470.

29. Guan, X., Nie, L., He, T., Yang, K., Xiao, T., Wang, S., Huang, Y., Zhang, J., Wang, J., Sharma, K., et al. (2014). Klotho suppresses renal tubulo-interstitial fibrosis by controlling basic fibroblast growth factor-2 signalling. J. Pathol. *234*, 560–572.

30. Kato, M., Zhang, J., Wang, M., Lanting, L., Yuan, H., Rossi, J.J., and Natarajan, R. (2007). MicroRNA-192 in diabetic kidney glomeruli and its function in TGF-beta-induced collagen expression via inhibition of E-box repressors. Proc. Natl. Acad. Sci. USA *104*, 3432–3437.

31. Zhou, Q., Fan, J., Ding, X., Peng, W., Yu, X., Chen, Y., and Nie, J. (2010). TGF-beta-induced MiR-491-5p expression promotes Par-3 degradation in rat proximal tubular epithelial cells. J. Biol. Chem. *285*, 40019–40027.

32. Wang, B., Komers, R., Carew, R., Winbanks, C.E., Xu, B., Herman-Edelstein, M., Koh, P., Thomas, M., Jandeleit-Dahm, K., Gregorevic, P., et al. (2012). Suppression of microRNA-29 expression by TGF-β1 promotes collagen expression and renal fibrosis. J. Am. Soc. Nephrol. *23*, 252–265.

33. Liu, L., Lin, W., Zhang, Q., Cao, W., and Liu, Z. (2016). TGF-β induces miR-30d down-regulation and podocyte injury through Smad2/3 and HDAC3-associated transcriptional repression. J. Mol. Med. (Berl.) *94*, 291–300.

34. Kou, X., Liu, X., Chen, X., Li, J., Yang, X., Fan, J., Yang, Y., and Chen, N. (2016). Ampelopsin attenuates brain aging of D-gal-induced rats through miR-34a-mediated SIRT1/mTOR signal pathway. Oncotarget *7*, 74484–74495.

35. Overstreet, J.M., Samarakoon, R., Meldrum, K.K., and Higgins, P.J. (2014). Redox control of p53 in the transcriptional regulation of TGF-β1 target genes through SMAD cooperativity. Cell. Signal. *26*, 1427–1436.

36. Jiang, L., Kon, N., Li, T., Wang, S.J., Su, T., Hibshoosh, H., Baer, R., and Gu, W. (2015). Ferroptosis as a p53-mediated activity during tumour suppression. Nature *520*, 57–62.

37. Valente, L.J., Gray, D.H., Michalak, E.M., Pinon-Hofbauer, J., Egle, A., Scott, C.L., Janic, A., and Strasser, A. (2013). p53 efficiently suppresses tumor development in the complete absence of its cell-cycle inhibitory and proapoptotic effectors p21, Puma, and Noxa. Cell Rep. *3*, 1339–1345.

38. Yugawa, T., Handa, K., Narisawa-Saito, M., Ohno, S., Fujita, M., and Kiyono, T. (2007). Regulation of Notch1 gene expression by p53 in epithelial cells. Mol. Cell. Biol. *27*, 3732–3742.

39. Yang, R., Xu, X., Li, H., Chen, J., Xiang, X., Dong, Z., and Zhang, D. (2017). p53 induces miR199a-3p to suppress SOCS7 for STAT3 activation and renal fibrosis in UUO. Sci. Rep. *7*, 43409.

40. Huang, Y., Chen, K., Ren, Q., Yi, L., Zhu, J., Zhang, Q., and Mi, M. (2018). Dihydromyricetin attenuates dexamethasone-induced muscle atrophy by improving mitochondrial function via the PGC-1α pathway. Cell. Physiol. Biochem. *49*, 758–779.

41. Liu, T.T., Zeng, Y., Tang, K., Chen, X., Zhang, W., and Xu, X.L. (2017). Dihydromyricetin ameliorates atherosclerosis in LDL receptor deficient mice. Atherosclerosis *262*, 39–50.

42. Henique, C., Bollée, G., Loyer, X., Grahammer, F., Dhaun, N., Camus, M., Vernerey, J., Guyonnet, L., Gaillard, F., Lazareth, H., et al. (2017). Genetic and pharmacological inhibition of microRNA-92a maintains podocyte cell cycle quiescence and limits crescentic glomerulonephritis. Nat. Commun. *8*, 1829.

43. Zanchi, C., Macconi, D., Trionfini, P., Tomasoni, S., Rottoli, D., Locatelli, M., Rudnicki, M., Vandesompele, J., Mestdagh, P., Remuzzi, G., et al. (2017). MicroRNA-184 is a downstream effector of albuminuria driving renal fibrosis in rats with diabetic nephropathy. Diabetologia *60*, 1114–1125.

44. Xue, M., Li, Y., Hu, F., Jia, Y.J., Zheng, Z.J., Wang, L., and Xue, Y.M. (2018). High glucose up-regulates microRNA-34a-5p to aggravate fibrosis by targeting SIRT1 in HK-2 cells. Biochem. Biophys. Res. Commun. *498*, 38–44.

45. Li, A., Peng, R., Sun, Y., Liu, H., Peng, H., and Zhang, Z. (2018). LincRNA 1700020I14Rik alleviates cell proliferation and fibrosis in diabetic nephropathy via miR-34a-5p/Sirt1/HIF-1α signaling. Cell Death Dis. *9*, 461.

46. Zhou, Y., Xiong, M., Niu, J., Sun, Q., Su, W., Zen, K., Dai, C., and Yang, J. (2014). Secreted fibroblast-derived miR-34a induces tubular cell apoptosis in fibrotic kidney. J. Cell Sci. *127*, 4494–4506.

47. Negri, A.L. (2005). The klotho gene: a gene predominantly expressed in the kidney is a fundamental regulator of aging and calcium/phosphorus metabolism. J. Nephrol. *18*, 654–658.

48. Doi, S., Zou, Y., Togao, O., Pastor, J.V., John, G.B., Wang, L., Shiizaki, K., Gotschall, R., Schiavi, S., Yorioka, N., et al. (2011). Klotho inhibits transforming growth factor-beta1 (TGF-beta1) signaling and suppresses renal fibrosis and cancer metastasis in mice. J. Biol. Chem. *286*, 8655–8665.

49. Satoh, M., Nagasu, H., Morita, Y., Yamaguchi, T.P., Kanwar, Y.S., and Kashihara, N. (2012). Klotho protects against mouse renal fibrosis by inhibiting Wnt signaling. Am. J. Physiol. Renal Physiol. *303*, F1641–F1651.

50. Yu, J., Deng, M., Zhao, J., and Huang, L. (2010). Decreased expression of klotho gene in uremic atherosclerosis in apolipoprotein E-deficient mice. Biochem. Biophys. Res. Commun. *391*, 261–266.

51. Lin, Y., Kuro-o, M., and Sun, Z. (2013). Genetic deficiency of anti-aging gene klotho exacerbates early nephropathy in STZ-induced diabetes in male mice. Endocrinology *154*, 3855–3863.

52. Koh, N., Fujimori, T., Nishiguchi, S., Tamori, A., Shiomi, S., Nakatani, T., Sugimura, K., Kishimoto, T., Kinoshita, S., Kuroki, T., and Nabeshima, Y. (2001). Severely reduced production of klotho in human chronic renal failure kidney. Biochem. Biophys. Res. Commun. *280*, 1015–1020.

53. Wu, F., Li, Y., Song, H., Zhang, Y., Zhang, Y., Jiang, M., Wang, F., Mu, Q., Zhang, W., Li, L., and Tang, D. (2016). Preventive effect of dihydromyricetin against cisplatin-induced nephrotoxicity in vitro and in vivo. Evid. Based Complement. Alternat. Med. *2016*, 7937385.

54. Wang, J.T., Jiao, P., Zhou, Y., and Liu, Q. (2016). Protective effect of dihydromyricetin against lipopolysaccharide-induced acute kidney injury in a rat model. Med. Sci. Monit. *22*, 454–459.

55. Baker, J.R., Vuppusetty, C., Colley, T., Papaioannou, A.I., Fenwick, P., Donnelly, L., Ito, K., and Barnes, P.J. (2016). Oxidative stress dependent microRNA-34a activation via PI3Kα reduces the expression of sirtuin-1 and sirtuin-6 in epithelial cells. Sci. Rep. *6*, 35871.

56. Bai, X.Y., Ma, Y., Ding, R., Fu, B., Shi, S., and Chen, X.M. (2011). miR-335 and miR-34a promote renal senescence by suppressing mitochondrial antioxidative enzymes. J. Am. Soc. Nephrol. *22*, 1252–1261.

57. Hermeking, H. (2007). p53 enters the microRNA world. Cancer Cell *12*, 414–418.

58. He, L., He, X., Lim, L.P., de Stanchina, E., Xuan, Z., Liang, Y., Xue, W., Zender, L., Magnus, J., Ridzon, D., et al. (2007). A microRNA component of the p53 tumour suppressor network. Nature *447*, 1130–1134.

59. Wei, C.L., Wu, Q., Vega, V.B., Chiu, K.P., Ng, P., Zhang, T., Shahab, A., Yong, H.C., Fu, Y., Weng, Z., et al. (2006). A global map of p53 transcription-factor binding sites in the human genome. Cell *124*, 207–219.

60. Yang, L., Besschetnova, T.Y., Brooks, C.R., Shah, J.V., and Bonventre, J.V. (2010). Epithelial cell cycle arrest in G2/M mediates kidney fibrosis after injury. Nat. Med. *16*, 535–543, 1p following 143.

61. Ying, Y., Kim, J., Westphal, S.N., Long, K.E., and Padanilam, B.J. (2014). Targeted deletion of p53 in the proximal tubule prevents ischemic renal injury. J. Am. Soc. Nephrol. *25*, 2707–2716.

62. Chen, S., Zhao, X., Wan, J., Ran, L., Qin, Y., Wang, X., Gao, Y., Shu, F., Zhang, Y., Liu, P., et al. (2015). Dihydromyricetin improves glucose and lipid metabolism and exerts anti-inflammatory effects in nonalcoholic fatty liver disease: a randomized controlled trial. Pharmacol. Res. *99*, 74–81.